Supporting information for

4-Dimensional modeling strategy for an improved understanding of miniemulsion NMP of acrylates initiated by SG1-macroinitiator

Paul H.M. Van Steenberge,[1,2] Dagmar R. D'hooge,[1,*] Marie-Françoise Reyniers,[1] Guy B. Marin[1], Michael F. Cunningham[2,*]

[1]Laboratory for Chemical Technology (LCT) Ghent University, Technologiepark 914, B-9052 Gent, Belgium

[2]Department of Chemical Engineering, Queen's University, Kingston, ON, K7L 3N6, Canada

Corresponding authors:

michael.cunningham@chee.queensu.ca and dagmar.dhooge@ugent.be

This Supporting Information contains:

1. Additional continuity and moment equations not specified in the main text.
2. The correlation used to account for diffusional limitations on termination.
3. Importance of chain transfer to monomer rate for Figure 1 and 5 in the main text and relevance of the non-"zero-one" nature of the studied miniemulsion NMP.
4. Detailed explanation of extrema in Figure 7 in the main text.

Continuity equations for integration of Smith-Ewart equations in the main text (Equation (1)) and the higher order moments equations for the calculation of the number average chain length and dispersity as a function of polymerization time

To calculate the number of particles having k secondary macroradicals, l nitroxide radicals, m initiator radicals, and n tertiary macroradicals ($N_{k,l,m,n}$) as a function of polymerization time t, the 4-dimensional Smith-Ewart equations (Equation (2) in the main text) must be complemented with continuity equations for the non-compartmentalized reactants, in agreement with the earlier work of Bentein *et al.* (reference 30 in the main text)

$$\frac{d[M]}{dt} = -[M]\left\{\left(k_{p0,s} + k_{tr_{rm}0,s}\right)\cdot[R_0] + \left(k_{p,s} + k_{tr_{rm},s}\right)\cdot[R_s] + \left(k_{p,t} + k_{tr_{rm},t}\right)\cdot[R_t]\right\} \tag{S.1}$$

$$\frac{d[R_0X]}{dt} = k_{da0,s}\left(\sum_{klmn}\frac{l}{N_A v_p}\cdot\frac{m}{N_A v_p}\cdot\frac{N_{k,l,m,n}}{N_p}\right) - k_{a0,s}[R_0X] \tag{S.2}$$

$$\frac{d[X]_{aq}}{dt} = \left(k_{exit,X}[X]\frac{v_p}{v_{aq}} - k_{entry,X}\frac{[X]_{aq}}{N_A v_{aq}}\right)N_p \tag{S.3}$$

$$\frac{d\tau_0}{dt} = k_{da,s}\left(\sum_{klmn}\frac{k}{N_A v_p}\cdot\frac{l}{N_A v_p}\cdot\frac{N_{k,l,m,n}}{N_p}\right) - k_{a,s}\tau_0 \tag{S.4}$$

$$\frac{d\omega_0}{dt} = k_{da,t}\left(\sum_{klmn}\frac{l}{N_A v_p}\cdot\frac{n}{N_A v_p}\cdot\frac{N_{k,l,m,n}}{N_p}\right) - k_{a,t}\omega_0 \tag{S.5}$$

in which the following average concentrations have been introduced for the compartmentalized species:

$$[R_0] = \frac{\bar{n}(R_0)}{N_A v_p} \qquad [R_s] = \frac{\bar{n}(R_s)}{N_A v_p} \qquad [R_t] = \frac{\bar{n}(R_t)}{N_A v_p} \qquad [X] = \frac{\bar{n}(X)}{N_A v_p}$$

Similarly, for the dead polymer and SCB branching amount the following equations can be derived:

$$\frac{d\mu_0}{dt} = \frac{1}{\left(N_A v_p\right)^2 N_p}\begin{pmatrix} k_{tc^0,s,app}\sum_{klmn} k\cdot m\cdot N_{k,l,m,n} + \\ k_{tc^0,t,app}\sum_{klmn} m\cdot n\cdot N_{k,l,m,n} + \\ k_{tc,ss,app}\sum_{klmn}(k-1)\cdot k\cdot N_{k,l,m,n} + \\ k_{tc,st,app}\sum_{klmn} k\cdot n\cdot N_{k,l,m,n} + \\ k_{tc,tt,app}\sum_{klmn}(n-1)\cdot n\cdot N_{k,l,m,n} \end{pmatrix} + [M]\left(k_{tr_{rm},s}[R_s] + k_{tr_{rm},t}[R_t]\right) \tag{S.6}$$

$$\frac{d[SCB]}{dt} = k_{p,t}[M][R_t] + \frac{1}{\left(N_A v_p\right)^2 N_p}\begin{pmatrix} k_{tc,st,app}\sum_{klmn} k\cdot n\cdot N_{k,l,m,n} + \\ 2k_{tc,tt,app}\sum_{klmn}(n-1)\cdot n\cdot N_{k,l,m,n} \end{pmatrix} \tag{S.7}$$

Furthermore, the number average chain length (x_n) and the dispersity are obtained by also integrating higher order moment equations although correcting for the compartmentalization of the zeroth order equations for bulk terms:

$$\begin{aligned} &\frac{d\lambda_1}{dt} = [M]\left(k_{p0,s}[R_0] + k_{p,s}[R_s] + k_{p,t,c}\nu_1\right) + k_{a,s}\tau_1 \\ &-\lambda_1\left(k_{tr_{rm},s,c}[M] + k_{tc,ss,app,c}[R_s] + k_{da,s,c}[X] + k_{tc^0,s,app,c}[R_0] + k_{tc,st,app,c}[R_t] + k_{bb}\right) \end{aligned} \tag{S.8}$$

$$\begin{aligned} &\frac{d\lambda_2}{dt} = [M]\left(k_{p0,s}[R_0] + k_{p,s}[R_s] + 2k_{p,s,c}\lambda_1 + k_{p,t}\nu_2\right) + k_{a,s}\tau_2 \\ &-\lambda_2\left(k_{tr_{rm},c}[M] + k_{tc,ss,app,c}[R_s] + k_{da,s,c}[X] + k_{tc^0,s,app,c}[R_0] + k_{tc,st,app,c}[R_t] + k_{bb}\right) \end{aligned} \tag{S.9}$$

$$\begin{aligned} &\frac{d\nu_1}{dt} = k_{bb}\lambda_1 + k_{a,t}\omega_1 \\ &-\nu_1\left(k_{p,t,c}[M] + k_{tr_{rm},t,c}[M] + k_{da,t,c}[X] + k_{tc,tt,app,c}[R_t] + k_{tc,st,app,c}[R_s] + k_{tc^0,t,app,c}[R_0]\right) \end{aligned} \tag{S.10}$$

$$\frac{d\nu_2}{dt} = k_{bb}\lambda_2 + k_{a,t}\omega_2 - \nu_2\left(k_{p,t,c}[M] + k_{tr_{rm},t,c}[M] + k_{da,t,c}[X] + k_{tc,tt,app,c}[R_t] + k_{tc,st,app,c}[R_s] + k_{tc^0,t,app,c}[R_0]\right) \quad \text{(S.11)}$$

$$\frac{d\tau_1}{dt} = k_{da,s,c}\lambda_1[X] - k_{a,s}\tau_1 \quad \text{(S.12)}$$

$$\frac{d\tau_2}{dt} = k_{da,s,c}\lambda_2[X] - k_{a,s}\tau_2 \quad \text{(S.13)}$$

$$\frac{d\mu_1}{dt} = [M]\left(k_{tr_{rm},s,c}\lambda_1 + k_{tr_{rm},t,c}\nu_1\right) + \left(k_{tc^0,s,app,c}\lambda_1 + k_{tc^0,t,app,c}\nu_1\right)[R_0] + \left(k_{tc,tt,app,c}\nu_1 + k_{tc,st,app,c}\lambda_1\right)[R_t] + \left(k_{tc,st,app,c}\nu_1 + k_{tc,ss,app,c}\lambda_1\right)[R_s] \quad \text{(S.14)}$$

$$\frac{d\mu_2}{dt} = \left(k_{tc,st,app,c}\nu_2 + k_{tc,ss,app,c}\lambda_2\right)[R_s] + \left(k_{tc^0,s,app,c}\lambda_2 + k_{tc^0,t,app,c}\nu_2\right)[R_0] + \left(k_{tr_{rm},s,c}\lambda_1 + k_{tr_{rm},t,c}\nu_1\right)[M] + \left(k_{tc,tt,app,c}\nu_2 + k_{tc,st,app,c}\lambda_2\right)[R_t] + k_{tc,st,app,c}2\lambda_1\nu_1 + k_{tc,ss,app,c}\lambda_1^2 + k_{tc,tt,app,c}\nu_1^2 \quad \text{(S.15)}$$

$$\frac{d\omega_1}{dt} = k_{da,t,c}\nu_1[X] - k_{a,t}\omega_1 \quad \text{(S.16)}$$

$$\frac{d\omega_2}{dt} = k_{da,t,c}\nu_2[X] - k_{a,t}\omega_2 \quad \text{(S.17)}$$

$$x_n = \frac{\tau_1 + \mu_1 + \lambda_1 + \omega_1 + \nu_1}{\tau_0 + \mu_0 + \lambda_0 + \omega_0 + \nu_0} \quad \text{(S.18)}$$

$$Dispersity = \frac{\left(\tau_1 + \mu_1 + \lambda_1 + \omega_1 + \nu_1\right)^2}{\left(\tau_0 + \mu_0 + \lambda_0 + \omega_0 + \nu_0\right)\left(\tau_2 + \mu_2 + \lambda_2 + \omega_2 + \nu_2\right)} \quad \text{(S.19)}$$

Diffusional limitations on termination

The following correlation is used to account for diffusional limitations on termination in a qualitative manner:

$$k_t = k_{t0} \exp(-0.4404\, w_{pol} - 6.362\, w_{pol}^{\ 2} - 0.1704\, w_{pol}^{\ 3}) \quad \text{(S.20)}$$

in which w_{pol} is the polymer mass fraction. This correlation was originally developed for styrene radical polymerizations but can be used to a first approximation in the current work, after correcting the value at zero conversion.

Importance of chain transfer and termination reactions

Figure S1 shows the various extensive rates of chain transfer to monomer and termination corresponding with Figure 1 in the main text, which distinguishes between $\Gamma = 50$ and $\Gamma = \infty$. It can be seen that in both cases mostly secondary chain transfer to monomer is responsible for the formation of dead polymer molecules and tertiary–tertiary termination is the most important termination reaction. It should however be stressed that the extensive rates in Figure S1 are not the most important rates as illustrated in Figure S2 for $\Gamma = 50$.

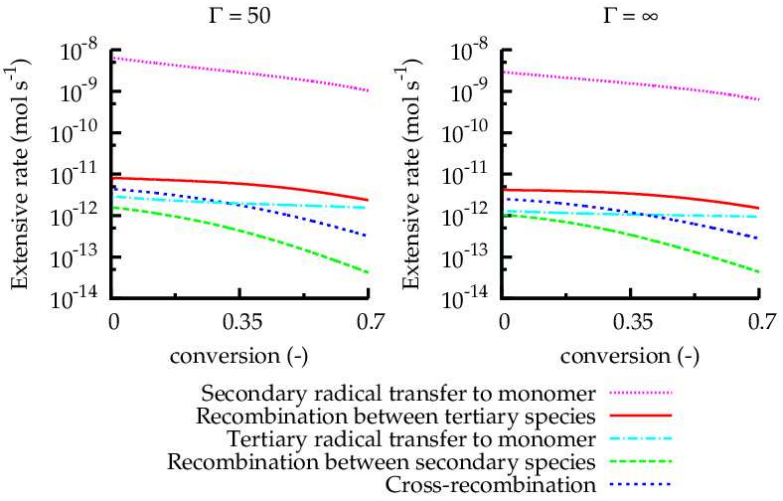

Figure S1: Extensive rates as specified in the legend for left: reference case with $\Gamma = 50$ and right: red dashed lines: $\Gamma = \infty$ for the NMP of *n*BuA in miniemulsion initiated by poly(*n*BuA)-SG1 macroinitiator ($[n\text{BuA}]_0$:$[\text{poly}(n\text{BuA})\text{-SG1}]_0 = 300$) at 393 K and for a d_p of 50 nm. Model parameters as given in Table 1 and 2 in the main text (Γ excepted); additional figure for Figure 1 in the main text.

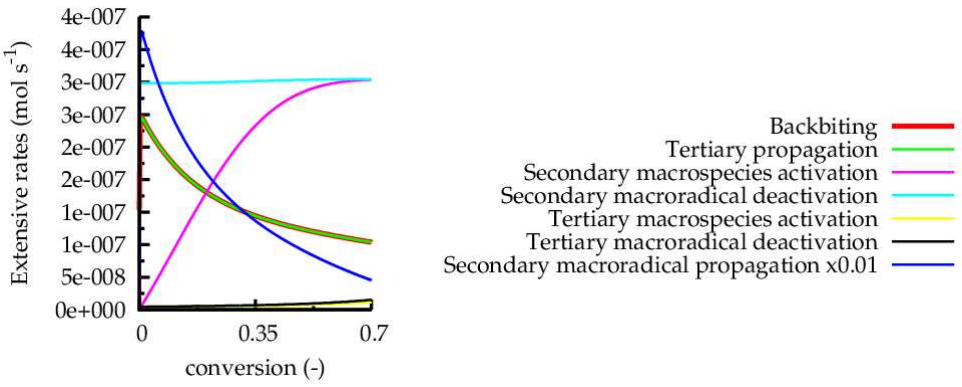

Figure S2: Additional extensive rates for Figure S1 (Γ = 50); note that for secondary propagation the rate is divided by 100.

Based on the extensive chain transfer rates in Figure S1, Figure S3 (left) can be constructed, which shows that for Γ = 50 more chain transfer takes place. A similar conclusion can be drawn for termination involving tertiary species (Figure S3, right).

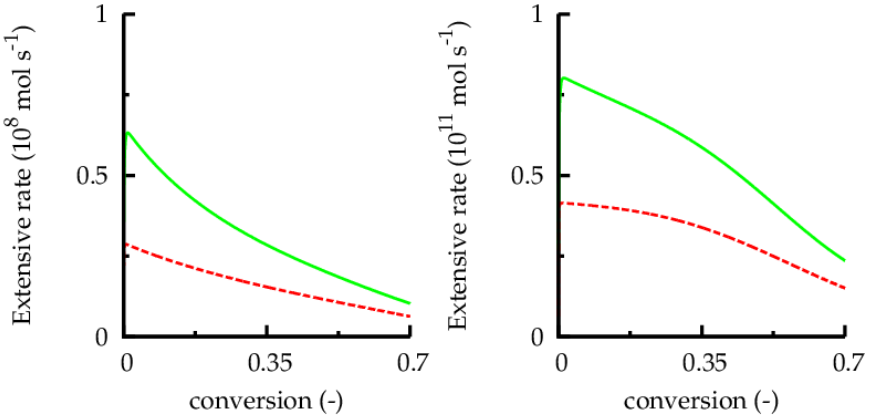

Figure S3: Left/right: Extensive secondary chain transfer to monomer/tertiary-tertiary termination rate with reference case with Γ = 50 (green full lines) and Γ = ∞ (red dashed lines) for the NMP of *n*BuA in miniemulsion initiated by poly(*n*BuA)-SG1 macroinitiator ($[n\text{BuA}]_0$:$[\text{poly}(n\text{BuA})\text{-SG1}]_0$ = 300) at 393 K and for a d_p of 50 nm. Model parameters as given in Table 1 and 2 in the main text (Γ excepted).

Figure S4 shows that this dominance for chain transfer to monomer is also the case if the termination reactivities are ten times increased compared to the values specified in Table 1 in

the main text. Note that such change results in a slower NMP and a better control over chain length (Figure S5). However, the conclusions as put forward in the main text remain valid.

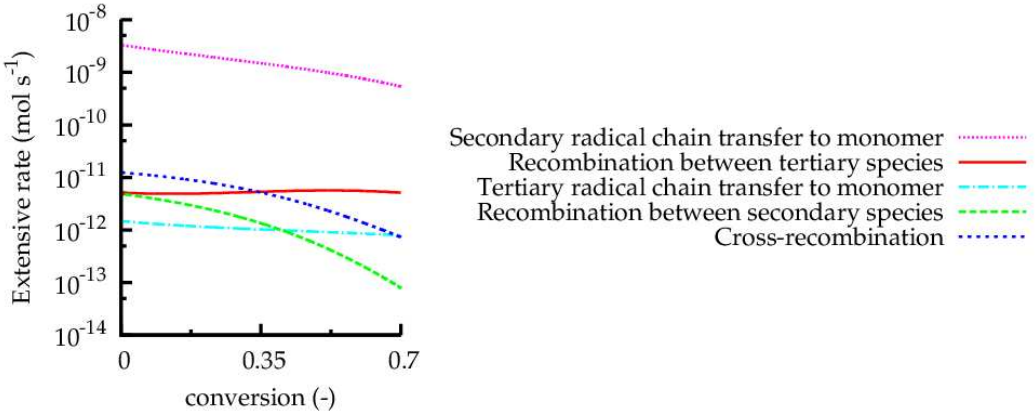

Figure S4: Extensive rates as specified in the legend: reference case but with ten times higher termination reactivity for the NMP of *n*BuA in miniemulsion initiated by poly(*n*BuA)-SG1 macroinitiator ([*n*BuA]$_0$:[poly(*n*BuA)-SG1]$_0$ = 300) at 393 K and for a d_p of 50 nm. Model parameters as given in Table 1 and 2 in the main text (the termination parameters and Γ excepted)

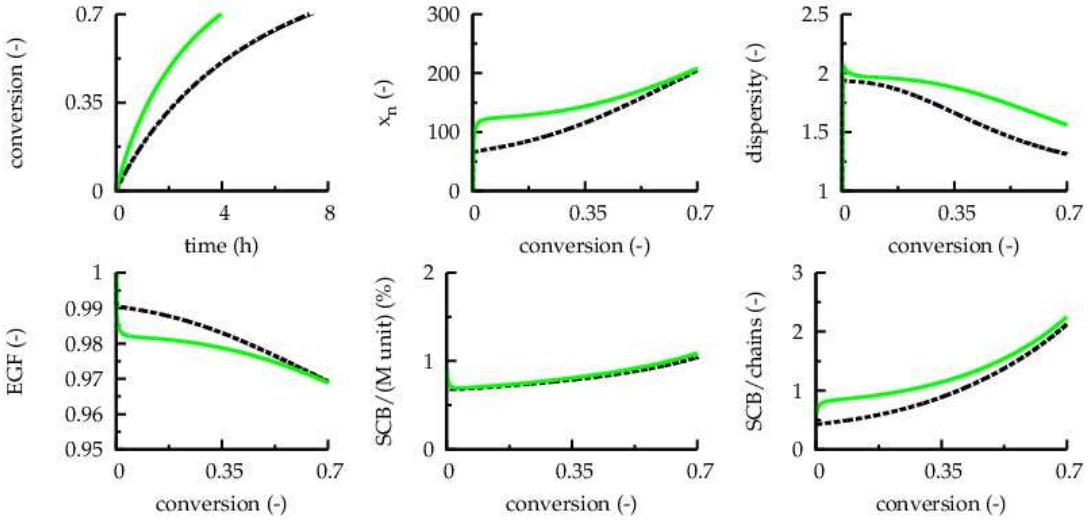

Figure S5: Comparison of simulation results accounting for termination as specified in Table 1 (green full lines) and increasing the termination rate coefficients with a factor 10 (black dashed lines) on the main polymer properties as a function of conversion for the NMP of *n*BuA in miniemulsion initiated by poly(*n*BuA)-SG1 macroinitiator ([*n*BuA]$_0$:[poly(*n*BuA)-SG1]$_0$ = 300) at 393 K and for a d_p of 50 nm. Model parameters as given in Table 1 and 2 (Γ = 50); x_n = number average chain length; EGF = end-group functionality; SCB = short chain branch; average chain length characteristics calculated ignoring the monomer units in the macro-initiator part.

Figure S6 (Γ = 50) highlights that despite the low termination rates, termination cannot be ignored for an accurate simulation of the NMP miniemulsion process. Clearly, different profiles for the main NMP characteristics are obtained in case termination is accounted for or neglected. In other words, the NMP miniemulsion cannot be described as a zero-one system.

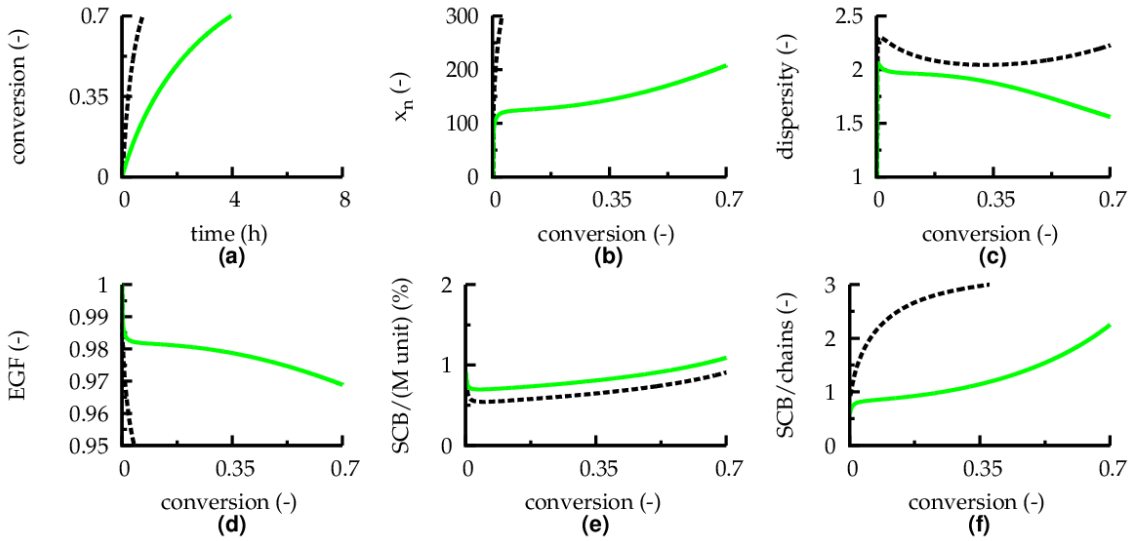

Figure S6: Comparison of simulation results accounting for termination (green full lines) and ignoring termination reactions (black dashed lines) on the main polymer properties as a function of conversion for the NMP of *n*BuA in miniemulsion initiated by poly(*n*BuA)-SG1 macroinitiator ($[n\text{BuA}]_0$:$[\text{poly}(n\text{BuA})\text{-SG1}]_0$ = 300) at 393 K and for a d_p of 50 nm. Model parameters as given in Table 1 and 2 (Γ = 50); x_n = number average chain length; EGF = end-group functionality; SCB = short chain branch; average chain length characteristics calculated ignoring the monomer units in the macro-initiator part.

Figure S7 shows the different chain transfer to monomer and termination extensive rates corresponding with Figure 5 in the main text, considering thus different values for the backbiting rate coefficient. Clearly, for a lower backbiting rate coefficient chain transfer to monomer involving secondary species is more important, explaining the lower EGF in Figure 5 upon a lowering of the backbiting rate coefficient.

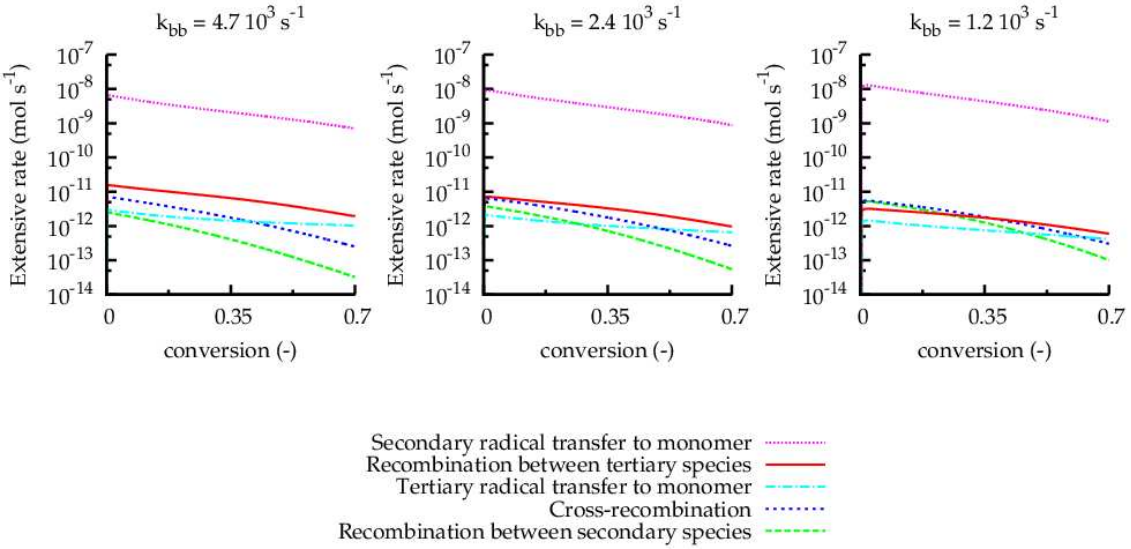

Figure S7: Effect of backbiting rate coefficient k_{bb} (25% (left), 50% (middle), 100% (right) of the value specified in Table 2) on extensive rates as specified in the legend. Model parameters as given in Table 1 and 2 in the main text (link with Figure 5).

Minimum for time and maximum for dispersity as a function of the particle diameter for low partitioning coefficients reactions

Figure S8a shows that at low particle diameters the ratio of the deactivation rate of NMP initiator to the corresponding activation rate increases. This results in a lower NMP initiator radical concentration (Figure S8b) and thus in a lower supply of new radicals (Figure S8c), as evidenced by the lower concentrations for the macroradicals in Figure S8d and Figure S8e. Hence, a lower polymerization rate is obtained and thus a better control over the chain length, explaining the extrema in Figure 7 in the main text.

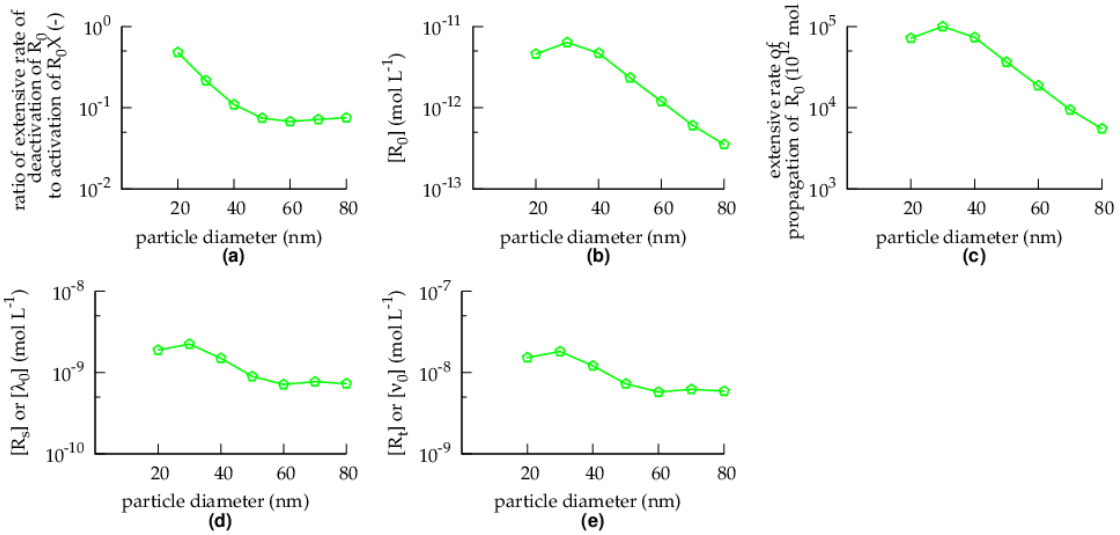

Figure S8: (a) Ratio of the extensive rate of deactivation to activation for initiator species, (b) the NMP initiator radical concentration, (c) the chain initiation rate, (d) the concentration of secondary radicals, (e) the concentration of tertiary radicals as a function of the particle diameter for the NMP of *n*BuA in miniemulsion initiated by poly(*n*BuA)-SG1 macroinitiator ($[n\text{BuA}]_0$:$[\text{poly}(n\text{BuA})\text{-SG1}]_0$ = 300) at 393 K; Γ = 50; conversion = 0.7.